Purification and Characterization of a Soluble Bioactive Amino-Terminal Extracellular Domain of the Human Thyrotropin Receptor†

Sabine Cornelis,‡ Sandrine Uttenweiler-Joseph,§ Valérie Panneels,|| Gilbert Vassart,‡,⊥ and Sabine Costagliola*,‡

IRIBHN and Department of Medical Genetics, ULB, Brussels, Belgium, Protein and Peptide Group, EMBL, Heidelberg, Germany, and Structural and Computational Biology Program, EMBL, Heidelberg, Germany

Received April 11, 2001; Revised Manuscript Received June 8, 2001

ABSTRACT: The amino-terminal ectodomain of the human TSH receptor has been expressed at the surface of CHO cells as a glycosylphosphatidylinositol-anchored molecule containing a 10-residue histidine tag close to its C terminus. The soluble ectodomain could be released from the cells by treatment with a glycosylphosphatidylinositol−phospholipase C and purified to apparent homogeneity by cobalt−Sepharose chromatography. Two nanomoles of material was obtained, which was suitable for analysis by mass spectrometry. This allowed the identification of four out of the six potential N-glycosylation sites as being effectively glycosylated. A proportion of the purified soluble ectodomain displayed specific binding of ^{125}I-labeled TSH, allowing for the first time performance of classical saturation binding experiments. Two classes of high-affinity binding sites were identified: site A, K_d 0.014 nM; site B, K_d 0.83 nM. The significance of site A, whose affinity is much higher than for the holoreceptor at the surface of intact cells, remains to be clarified. The purified ectodomain was capable of inhibiting efficiently the thyroid stimulating activity of immunoglobulins from patients with Graves' disease. It allowed computation of the amounts of these immunoglobulins in patient's serum, giving values up to 10 μg/mL. Contrary to all currently available assays, the soluble ectodomain of the TSH receptor purified in a functionally competent conformation allows direct studies of its interactions with TSH and autoantibodies and opens the way to structural studies.

The thyrotropin receptor (TSHr),[1] like the other members of the glycoprotein hormone receptor family (FSH and LH/hCG receptors), displays a bipartite structure, with a large amino-terminal extracellular domain (ECD) responsible for high-affinity hormone binding and a serpentine carboxyl-terminal portion, characteristic of the opsin family of G protein-coupled receptors (*1*−*3*). The ECD is structurally related to the leucine-rich repeats (LRR) superfamily of proteins, and 3-D structural models have been proposed for both the TSHr and the LH/CGr ectodomains (*4*, *5*) on the basis of the crystal structure of porcine ribonuclease inhibitor, the first LRR protein whose 3-D structure has been solved (*6*). Recently, Remy et al. reported the expression and purification of a soluble hCG/ECD LHr complex secreted by CHO cells and confirmed by circular dichroism that the structure was in agreement with the helix and β sheet content predicted in the models (*7*).

The structural and functional dichotomy between hormone binding and stimulation of the serpentine domain of glycoprotein hormone receptors poses the interesting question of the mechanism involved in the intramolecular transduction of the activation signal. Whereas in receptors belonging to the metabotropic glutamate receptor family (another GPCR family with large amino-terminal domains responsible for binding of the agonists) activation involves a dimerization of the ligand-binding region (*8*), the phenotype of natural mutants and site-directed mutagenesis experiments have led to the notion that the ectodomain of the TSHr would exert a silencing effect on the serpentine portion of the molecule (*9*−*11*). The mechanisms implicated in switching this inhibitory interaction into stimulation upon binding of the hormone remain unknown.

Also, the TSHr presents the peculiarity of being stimulated by autoantibodies present in the plasma of patients with Graves' disease (reviewed in ref *12*). It is known that stimulating antibodies (TSAbs) target the ectodomain of the receptor, but the precise epitopes involved and the mechanism leading to activation of the serpentine domain are unknown. Availability of the amino-terminal ectodomain of the TSHr in a soluble and bioactive form would constitute an invaluable tool to approach all of these problems.

† This study was supported by the Belgian State, Prime Minister's Office, Service for Sciences, Technology and Culture, and also supported by grants from the FRSM, FNRS, Association Recherche Biomedicale et Diagnostic, and BRAHMS Diagnostics. S. Costagliola and S. Cornelis are Chercheur Qualifié at the FNRS and fellow of FRIA, respectively.

* To whom correspondence should be addressed: IRIBHN, ULB, Campus Hôpital Erasme, bâtiment C, 808 route de Lennik, B-1070 Bruxelles, Belgium. Phone: 32 2 555.41.97. Fax: 32 2 555.46.55. E-mail: scostag@ulb.ac.be.

‡ IRIBHN, ULB.

§ Protein and Peptide Group, EMBL.

|| Structural and Computational Biology Program, EMBL.

⊥ Department of Medical Genetics, ULB.

[1] Abbreviations: TSAb, thyroid stimulating antibody; TSBAb, thyroid stimulating blocking antibody; TBII, thyroid stimulating binding inhibition immunoglobulin; ECD, extracellular domain; TSHr, thyroid stimulating hormone receptor; TSH, thyrotropin; LRR, leucine-rich repeat; GPI, glycosylphosphatidylinositol; PI-PLC, GPI-specific phospholipase C; PEG, poly(ethylene glycol).

10.1021/bi0107389 CCC: $20.00
Published on Web 07/24/2001

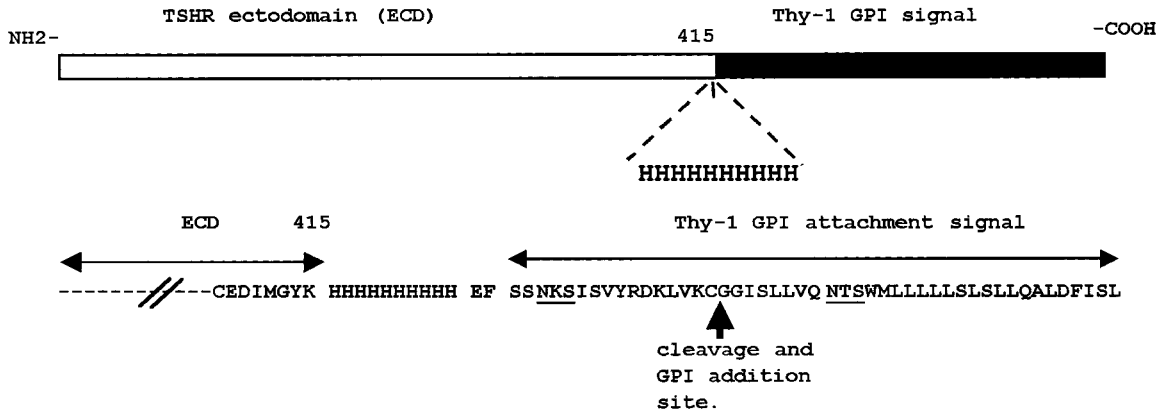

FIGURE 1: Schematic representation of the GPI-anchored TSHr-ECD chimeric protein. The C-terminal part of the chimeric Thy-1 TSHr-ECD construct is shown; fusion is realized after position 415 of the TSHr, with two intervening amino acids (EF) preceding a stretch of 10 histidines and 53 residues of the mouse Thy-1 molecule responsible for GPI anchor addition. Two potential sites of N-glycosylation (NKS and NTS) introduced with the Thy-1 GPI attachment signal are underlined.

Attempts to express the ECD of the TSHr as a soluble molecule capable of binding TSH with high affinity have met with difficulties. After exploring a series of strategies, in acellular systems (*13*, *14*), in procaryotes (*15*−*19*), in insect cells (*20*−*23*), or in mammalian cells (*24*−*30*), only recently has it been possible to produce some bioactive material. Successful approaches exploited expression of the ectodomain at the surface of CHO cells via anchoring by a glycosylphosphatidylinositol (GPI) moiety (*29*, *30*), as a chimeric molecule containing a single transmembrane segment of the CD8 protein (*26*, *27*), or a more confusing report, using a vaccinia virus system, but in this case the ectodomain was not secreted (*31*). In the former experiments soluble ectodomain was released from the cells by a GPI-specific phospholipase C (PI-PLC); in the latter, by cleavage of a thrombin site engineered in the construct at the border between the ectodomain and the transmembrane segment. In a different experimental setting, a truncated TSHr ectodomain containing the first 261 amino acids was shown to bind efficiently TSAbs but was devoid of TSH binding activity (*28*). The production of soluble material displaying the binding characteristics of the holoreceptor and allowing for the determination of the basic binding parameters of the ECD in standard in vitro binding experiments has not been described so far. Building on previous data, we have succeeded in purifying a large amount of the GPI-anchored extracellular domain of the TSHr after release from the cell surface by phospholipase C. Two nanomoles of highly purified ECD was obtained in a form capable of binding Graves' autoantibodies and, for a fraction of it, TSH. Purity of the material allowed direct identification by mass spectrometry of asparagine residues implicated in glycosylation of the ectodomain.

EXPERIMENTAL PROCEDURES

Reagents. The BA8 monoclonal antibody recognizing a conformational epitope on the TSHr extracellular domain has been described elsewhere (*32*). The 3G4 monoclonal antibody, recognizing a linear epitope on the TSHr ectodomain (VFFEEQE, residues 354−360), was obtained using the same genetic immunization approach. Iodinated bTSH (bioactivity 50−60 TSH IU/mg; specific radioactivity 58 μCi/μg) was a kind gift from BRAHMS Diagnostica (Berlin).

Construction of TSHr ECD with a 10 Histidine Tag and a GPI Anchor. A 170 bp fragment encoding the signal peptide for GPI addition at the C terminus of mouse Thy-1 cDNA and contained in plasmid pTM813 (*33*) was PCR-amplified using the upstream primer 5′-TTAGAATTCAG-CTCCAATAAAAGTATCAGTGTGTA-3′ and the downstream primer 5′-ATTGGATCCTCACAGAGAAATGAA-GTCTAGG-3′. The PCR product was digested with *Eco*RI and *Bam*HI and inserted into the prokaryotic vector SK+. The resulting construct was digested with *Eco*RV and *Eco*RI, and a double-stranded oligonucleotide adapter encoding DIMGYKHHHHHHHHHHEF (see Figure 1) was inserted [upper strand, 5′-ATCATGGGCTACAAG$(CAT)_{10}$G-3′; lower strand, 5′-AATTC$(ATG)_{10}$CTTGTAGCCCATGAT-3′]. An *Eco*RV site was engineered by site-directed mutagenesis in position 1230 of the ectodomain of human TSHr. The resulting ECD construct, in SK+, was excised with *Xho*I/*Eco*RV and fused upstream of the segment encoding the signal for GPI addition. The TSHr-ECD-10His construct with its signal for GPI attachment is illustrated in Figure 1. This construct was then subcloned in pEFIN, a bicistronic vector developed at EUROSCREEN (Brussels, Belgium) for stable transfection in CHO cells.

Generation of a Stable CHO Cell Line (ECD-10His) Expressing the ECD-10His-GPI. The pEFIN vector harboring the TSHr-ECD-10His containing the Thy-1 signal for GPI addition was transfected in CHO-K1 cells as described (*30*). Stable cell lines were selected by resistance to Geneticin, and one clone (ECD10His), with the highest expression of the ECD at the plasma membrane, was selected by flow cytometry using the BA8 antibody and anti-His antibody (H 1029, Sigma-Aldrich, Brussels, Belgium) and characterized for TSH binding as described for the GPI-ECD cell line GT14 (*30*).

Production and Purification of Recombinant PI-PLC. For expression of the PI-PLC under the control of the *lac-tac-tac* triple promoter, a culture of *Escherichia coli* MM294 harboring the plasmid pIC, containing the cDNA coding for the PI-PLC from *Bacillus cereus* (this construction was a kind gift from Dr. O. Hayes Griffith, Institute of Molecular Biology, University of Oregon, Eugene, OR, was grown and induced by IPTG as described by Koke et al. (*34*). Cells were harvested by centrifugation, and PI-PLC was recovered

as described (*34*) and analyzed by SDS−PAGE and Coomassie blue staining. Enzyme activity was measured by incubation with cells expressing the ECD-GPI protein [GT14 cells (*30*)]. The relative amount of ECD released from the cell surface was estimated by FACS with BA8 antibody (*32*) or by ^{125}I-TSH binding as already described (*30*).

Purification of the TSHr Ectodomain (ECD). 10^9 CHO ECD-10His cells were washed three times with Dulbecco's modified Eagle's medium and incubated overnight with PI-PLC in culture medium without serum. The supernatant (500 mL) was harvested, centrifuged, and concentrated 100 times using a stirred ultrafiltration cell (Amicon, Beverly, MA). This concentrated supernatant was used without any further purification for binding experiments with TSH and autoantibodies. For SDS−PAGE analysis, the supernatant was diluted 10 times in the binding buffer (Tris, 20 mM, pH 8, NaCl, 500 mM, Triton X-100, 0.1%) and concentrated 100 times using an Ultrafree centrifugal filter (Millipore Corp., Bedford, MA). Imidazole (5 mM final concentration) was added to the resulting 2−4 mL of concentrated supernatant, which was then incubated with an equilibrated cobalt-based immobilized metal affinity chromatography (IMAC) resin (*35*) (TALON Clontech, Palo Alto, CA) at 4 °C during 30 min under agitation. After extensive washing with binding buffer containing 5 mM imidazole, the resin was finally loaded onto a small glass spin column. Bound material was eluted in 100 μL fractions, with binding buffer containing an increasing amount of imidazole (from 10 to 500 mM). Samples were analyzed by SDS−PAGE and western blotting with 3G4 antibody, as already described (*30*), or by direct staining with Coomassie blue.

Binding of [^{125}I]TSH. Concentrated culture supernatant of 10^9 ECD-10His CHO cells (2.5 μL) treated with PI-PLC was diluted to a final volume of 100 μL in a Hepes−phosphate buffer (Hepes, 20 mM, KH_2PO_4, 0.44 mM, Na_2HPO_4, 0.33 mM, KCl, 5.4 mM, BSA 0.05%, pH 7.4). One hundred microliters of various amounts of radioactive TSH diluted in a Hepes buffer (Hepes, 10 mM, Triton X-100, 0.1%, $CaCl_2$, 20 mM, heparin, 20 000 units/L, BSA, 2%), imidazole (5 mM final concentration), and 5 μL of nickel magnetic beads (Ni−NTA magnetic agarose beads, QIAGEN, Valencia, CA) were added and incubated for 4 h at room temperature under agitation. Tubes were placed on a magnetic separator for 1 min, and the supernatant was removed with a pipet. Beads were washed twice with 500 μL of ice-cold washing buffer (Hepes, 100 mM, Triton X-100, 0.1%, imidazole, 20 mM, pH 7.4), and radioactivity was measured in a γ counter. All experiments were done in triplicate, and results are expressed as cpm bound. The nonspecific binding was measured in the presence of 500 nM cold TSH.

Neutralization of TSHr Autoantibodies in the Serum of Graves' Patients. Thyroid stimulating activity in serum from patients with Graves' disease was measured using CHO cells expressing the human TSHr, JP26 (*36*), in the presence of various amounts of soluble ECD. Briefly, 3×10^5 cells per 3 cm plate were incubated in Krebs−Ringer−Hepes buffer (KRH) (124 mM NaCl, 5 mM KCl, 1.25 mM KH_2PO_4, 1.25 mM $MgSO_4$, 1.45 mM $CaCl_2$, 25 mM Hepes, pH 7.4, 8 mM glucose), supplemented with 25 μM rolipram (a cyclic AMP phosphodiesterase inhibitor; Laboratoire Logeais, Paris), 0.1% BSA, and 50 μL of patient's serum which had been preincubated for 30 min with various amounts of soluble ECD (total volume, 1 mL per plate). At the end of 1 h incubation, the medium was discarded and replaced with 0.1 M HCl. The cell extracts were dried in a vacuum concentrator, resuspended in water, and diluted appropriately for cyclic AMP measurements by RIA according to the method of Brooker (*37*). Duplicate samples were assayed in all experiments; results are expressed as picomoles of cAMP per milliliter.

Determination of the N-Glycosylation Sites of TSHr. (A) Deglycosylation in the Presence of ^{18}O. Twenty picomoles of TSHr ectodomain was denatured for 10 min at 100 °C in 5% SDS−10% β-mercaptoethanol. Twenty microliters of the deglycosylation buffer (100 mM phospate buffer, pH 7.5, EDTA, 40 mM, Triton, 2%), half diluted with $H_2{}^{18}O$ (Phychem, Düren, Germany), was added together with 2 units of PGNase F (Boehringer Mannheim, Mannheim, Germany). The reaction mixture was left overnight at 37 °C. The deglycosylated sample was run on standard 1-D SDS−PAGE and visualized by Coomassie blue.

(B) In-Gel Digestion of the Deglycosylated TSHr. Before in-gel digestion with trypsin, the deglycosylated TSHr ectodomain was reduced and S-alkylated with iodoacetamide essentially as described (*38*).

(C) MALDI MS Peptide Mass Mapping and Peptide Sequencing by Nanoelectrospray Tandem Mass Spectrometry. The in-gel digest mixture (0.4 μL) was applied on a matrix surface made by the fast evaporation method (*39*). MALDI mass spectra were acquired on a modified Bruker Reflex reflectron TOF mass spectrometer as described (*38*) (Bruker-Franzen, Bremen, Germany). The supernatant containing the peptides obtained by in-gel proteolysis was collected, and the gel pieces were further extracted with 50% acetonitrile. All extracts were pooled and dried in a vacuum. For analysis, the peptide mixture was taken up in 1 μL of 80% formic acid and rapidly diluted with 9 μL of water. The peptide mixture was desalted on self-assembled Poros R2 and R3 columns and eluted using two times 1 μL of 60% methanol−5% formic acid directly into a nanoelectrospray needle (*38*, *40*). Samples were analyzed with the Q-TOF1 mass spectrometer equipped with the nanoelectrospray ion source (Micromass, Manchester, U.K.). For every tandem mass spectrometric analysis, the transmission window was adapted to select the complete isotopic pattern of the desired ion, and the collision energy was adjusted for each peptide.

RESULTS

Characterization of the ECD-10His Cell Line. The 10His tag was fused at position 415 of the TSH receptor (see Experimental Procedures and Figure 1) before the 53 amino acid signal peptide for GPI anchor addition. The construct was transfected in CHO cells, and one cell line (ECD-10His) expressing particularly high levels of ECD at the cell surface was selected by flow cytometry using BA8 (Figure 2A), a monoclonal antibody recognizing a conformational epitope of the ECD (*32*), and a monoclonal anti-His antibody (Figure 2B). These results showed that the His tag did not interfere with targeting of the construct to the plasma membrane and was accessible to antibody. Consequently, it was expected that the His-tagged ectodomain would be amenable to metal−chelate affinity chromatography, with no need to

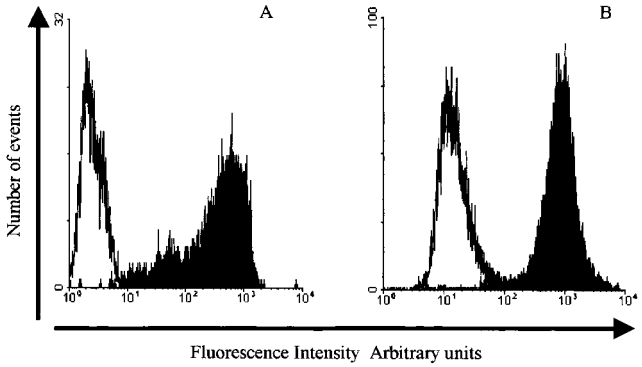

FIGURE 2: Analysis of cell surface expression of the GPI-anchored ectodomain by flow cytofluorometry. (A) Histograms of fluorescence intensity showing the binding of the BA8 antibody to a CHO line expressing the GPI-anchored TSHr-ECD-10His (black histogram) or no receptor (open histogram). (B) Histograms of fluorescence intensity showing the binding of the anti-His monoclonal antibody to a CHO line expressing the GPI-anchored TSHr-ECD-10His (black histogram) or no receptor (open histogram).

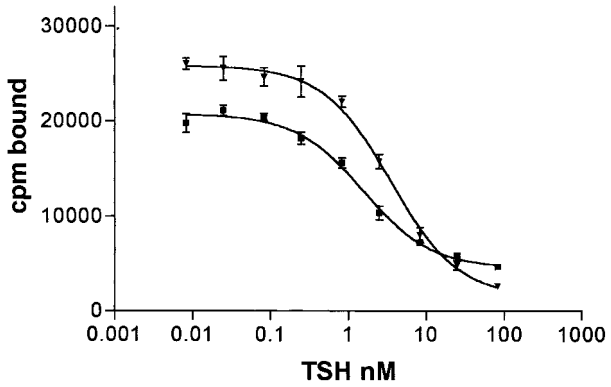

FIGURE 3: TSH binding to GPI-anchored TSHr-ECD in intact cells. CHO lines expressing the GPI-anchored TSHr-ECD-10His (■) or full length holoreceptor (JP19 cells) (▼) in 3 cm dishes were incubated with 100 000 cpm of ^{125}I-bTSH and varying concentrations of cold bTSH. Each point was tested in triplicate, and the results are expressed as bound radioactivity. The data were analyzed with GraphPad Prism (GraphPad Software, Inc., San Diego, CA) which fit the data to a one-site competitive binding curve.

denature the protein. Interaction with the BA8 mAb, which interacts only with native forms of TSHr (*32*), emphasized the correctly folded structure of the ECD-10His GPI protein. This point was confirmed by TSH binding experiments. Intact ECD-10His cells bind ^{125}I bovine TSH with an affinity similar to that of CHO cells [JP19, (*36*)] expressing the holoreceptor (K_d 1.56 vs 3.5 nM for ECD-10His and JP19 cells, respectively) **(**Figure 3**)**. Estimation of the number of TSHr/cell from analysis of the binding curves gave numbers in excess of 10^6.

Production and Purification of the ECD. Batches of 10^9 ECD-10His CHO cells were treated with PI-PLC, and the material released from the cells was purified on a cobalt-based IMAC column as described under Experimental Procedures. The eluted material was analyzed by SDS−PAGE and Coomassie blue staining (Figure 4). In the fractions eluting between 50 and 100 mM (*32*) imidazole, a strongly stained but fuzzy band, characteristic of a glycosylated protein, was visualized at the expected size (95 kDa) (*30*) with no obvious contaminants. The purified material was quantified by the Bradford method, yielding a total protein amount of 150 μg. Western blotting and immunodetection with 3G4 antibody, directed against a linear epitope of the ECD, confirmed that the purified protein was the TSHr-ECD (Figure 5).

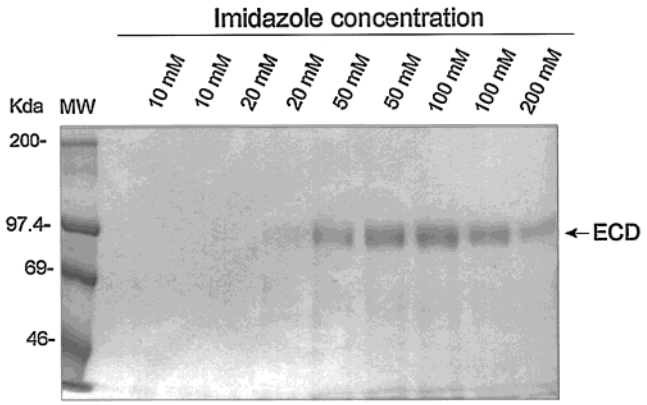

FIGURE 4: ECD-10His purification. The concentrated supernatant of CHO ECD-10His treated with PI-PLC was incubated with an equilibrated cobalt-based immobilized metal affinity chromatography (IMAC) resin. After extensive washing with binding buffer (described in Experimental Procedures) containing 5 mM imidazole, the resin was loaded onto a glass spin column. Bound material was eluted in 100 μL fractions with binding buffer containing increasing amounts of imidazole (from 10 to 500 mM). Five microliters of each fraction was analyzed by SDS−PAGE under reducing conditions.

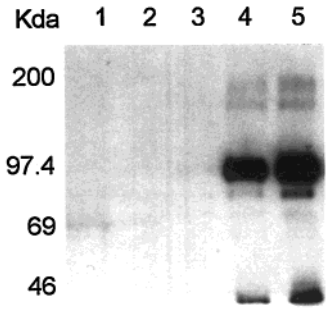

FIGURE 5: Analysis of ECD-10His by immunoblotting. Aliquots of purified ECD-10His eluted with different amounts of imidazole were resuspended in SDS−PAGE−β-mercaptoethanol loading buffer and analyzed by immunoblotting with the 3G4 antibody. Lanes: 1, column flow-through; 2−5, ECD-10His eluted with 10, 20, 50, and 100 mM imidazole, respectively.

Determination of N-Glycosylation Sites of TSHr. Twenty picomoles of purified ECD was treated with *N*-glycosidase F to remove all N-linked sugar moieties. As described in Experimental Procedures, this deglycosylation step was performed in the presence of $H_2{}^{18}O$ in order to label the N-glycosylation sites with ^{18}O. After separation by SDS−PAGE and in-gel digestion with trypsin, the resulting tryptic peptides of the deglycosylated ECD were analyzed by MALDI and nanoESI-MS (see Experimental Procedures). Three tryptic peptides containing the putative N-glycosylation sites in positions 77, 113 and 302 (peptides TIPSHAFSN-LP**NIS**R, **NLT**YIDPDALK, and GILESLMC**NES**SMQSLR with C corresponding to alkylated cysteine) were observed by MALDI with a mass shift of 1 Da (due to the Asn to Asp conversion associated with the deglycosylation step) and as double peaks with a 2 Da spacing characteristic of the ^{18}O labeling (Figure 6 and Table 1). These three peptides were also seen by ESI-MS as well as a fourth tryptic peptide containing the N-glycosylation site in position 198 (LYN-NGFTSVQGYAF**NGT**K) (Table 1 and Figure 7A). The

FIGURE 6: Summary of the determination by mass spectrometry of N-glycosylation sites of the ECD-10His protein. The theoretical tryptic peptides containing the putative N-glycosylation sites (in bold) are underlined. After deglycosylation in the presence of $H_2{}^{18}O$ and in-gel tryptic digestion, three of these peptides were observed by MALDI and nanoESI-MS with a mass shifted by 1 Da because of the N to D conversion resulting from the deglycosylation step and the doublets of peaks due to the incorporation of ^{18}O (see Experimental Procedures). A fourth peptide was only observed by nanoESI-MS, and all these peptides were sequenced by nanoESI-MS/MS to confirm the glycosylation site. Two tryptic peptides with the putative N-glycosylation sites in positions 99 and 177 were not observed by MALDI or nanoESI-MS.

Table 1: Detection by Mass Spectrometry of the Tryptic Peptides from ECD Containing the Putative N-Glycosylation Sites[a]

tryptic peptides with putative N-glycosylation site	MALDI-TOF MS (monoisotopic MH^+)	ESI-Q-TOF MS (Figure 7A) [monoisotopic $(M + 2H)^{2+}$]
NLTYIDPDALK (1261.65 Da)	$MH^+ = 1263.48$	$(M + 2H)^{2+} = 632.29$
TIPSHAFSNLP**NIS**R (1652.86 Da)	$MH^+ = 1254.73$	$(M + 2H)^{2+} = 827.88$
GILESLMC**NES**SMQSLR (1953.89 Da)	$MH^+ = 1971.84$ (Mox) $MH^+ = 1987.86$ (2Mox)	$(M + 2H)^{2+} = 978.40$
LYNNGFTSVQGYAF**NGT**K (1979.93 Da)	ND	$(M + 2H)^{2+} = 991.89$ (deamidation of an N)
IYVSIDVTLQQLESHSFY**NLS**K (2583.32 Da)	ND	ND
VYSTDIFFILEITDNPYMTSIPVNAFQGLC**NET**LTLK (4281.13 Da)	ND	ND

[a] After deglycosylation in the presence of $H_2{}^{18}O$ (where the N to D conversion of the N-glycosylation site takes place), the ECD is digested with trypsin (after alkylation of the cysteine residues), and the resulting peptides are analyzed by MALDI-TOF and ESI-Q-TOF mass spectrometry (Figure 7A). Because the ionization process of MALDI and ESI is different, some peptides present in the mixture are sometimes observed with only one of these MS techniques.

glycosylation sites of these four peptides were confirmed by MS/MS sequencing as illustrated in Figure 7B. No peak was detected by MALDI or nanoESI-MS which could correspond to either the deglycosylated or unglycosylated tryptic peptides containing the putative N-glycosylation sites in positions 99 and 177 (Figure 6 and Table 1).

Binding of TSH on the Soluble ECD. To study the interaction of TSH with ECD, we established a new binding assay (see Experimental Procedures) in which the TSH−ECD complex was separated from free TSH by nickel−agarose magnetic beads. After determination of the kinetics of the binding reaction (equilibrium approached after 240 min; see Figure 8A), the assay allowed for the first time estimation of the dissociation constant (K_d) of TSH for the soluble ECD from a classical saturation binding curve (Figure 8B). An interesting characteristic of the assay is the very low nonspecific binding it displays, allowing for precise estimation of binding parameters. The minimal model giving an acceptable fitting of the specific binding data requires two classes of binding sites according to the equation:

$$Y = B_{max1}X/(K_{d1} + X) + B_{max2}X/(K_{d2} + X)$$

$P = 0.7331$ (P value >0.5 indicated that the data follow the equation selected); site A, $K_d = 0.014 \pm 0.04$ nM and $B_{max} = 0.007 \pm 0.002$ nM; site B, $K_d = 0.83 \pm 0.09$ nM and $B_{max} = 0.05 \pm 0.005$ nM (the experimental variations for the K_d and B_{max} values were calculated from three independent experiments). The amount of bioactive ECD capable of binding TSH in the range of TSH concentrations used

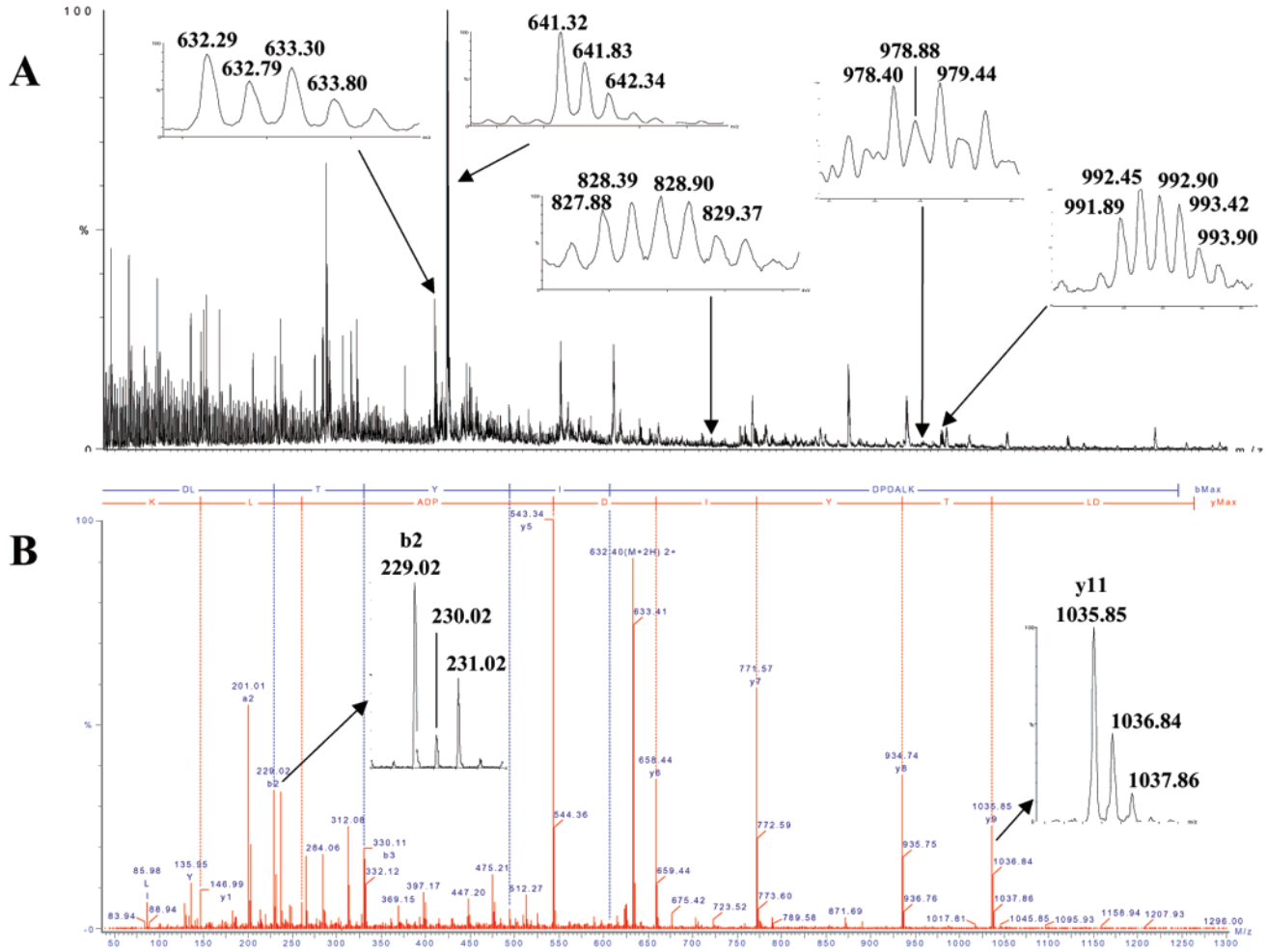

FIGURE 7: NanoESI-MS and MS-MS experiments for the determination of the N-glycosylation sites of the ECD-10His protein. After deglycosylation in the presence of $H_2{}^{18}O$ and in-gel tryptic digestion, the resulting proteolysis mixture was analyzed by nanoESI-MS (A). The insets represent the isotopic profiles of doubly charged ions corresponding to different tryptic peptides. The unlabeled tryptic peptide IPSLPPSTQTLK (position 47−58) with a monoisotopic *m*/*z* at 641.32 displays a classical isotopic profile. The other ions have an isotopic profile characteristic of the ^{18}O labeling and correspond to the following tryptic peptides which were N-glycosylated as confirmed by the N to D conversion: **DLT**YIDPDALK with $(M + 2H)^{2+} = 632.29$, TIPSHAFSNLP**DIS**R with $(M + 2H)^{2+} = 827.88$, GILESLMC**DES**SMQSLR with $(M + 2H)^{2+} = 978.40$, and LYN**D**FGTSVQGYAF**DGT**K with $(M + 2H)^{2+} = 991.89$ (the D in bold results from a deamination of N, deamination which can occur during the denaturation step performed at high temperature). The glycosylation sites of these peptides were confirmed by MS-MS sequencing as illustrated in (B) for the tryptic peptide **DLT**YIDPDALK.

represents only a proportion (ca. 5%) of the total amount of ECD (see Discussion).

Binding of Autoantibodies to Soluble ECD. The ability of the soluble ECD to neutralize the thyroid stimulating activity (TSAb) of serum from patients with Graves' disease was measured using CHO cells expressing the wild-type holoreceptor (JP26) (*36*). The cells were incubated with five sera with a very high TSAb activity, which had been preincubated or not in the presence of 3 μg of soluble ECD (Figure 9A), and the cAMP produced was measured. The soluble ECD neutralized efficiently the TSAb activity (95%−100% inhibition) in the five sera tested. Experiments with increasing amounts of soluble ECD showed that a concentration of 500 ng/mL (5 nM) was necessary to neutralize 50% of the autoantibody activity (Figure 9B) present in 50 μL of serum from the patient with the highest TSAb activity.

DISCUSSION

Production of the ectodomain of the TSHr according to the present protocol presents a series of advantages over previous protocols. It essentially allows preparation of sizable amounts of soluble highly purified material presenting the functional characteristics of the native domain, as it is when part of the holoreceptor. Compared with the relatively easy production of the ectodomain of the LH/CG receptor (*7*, *15*), attempts to prepare soluble ectodomain of the TSHr has been exceptionally difficult: most simple strategies led to trapping of denatured material within the cells or to production of protein devoid of TSH binding activity (*25*, *28*, *41*). Recently, three strategies yielded more promising results: Rapoport's group, by truncating the ECD after residue 261, could obtain a His-tagged soluble ectodomain presenting very efficient TSAb binding activity but incapable of binding TSH (*28*). It is likely that additional downstream residues are involved in TSH binding or are required to stabilize the three-dimensional structure of the ectodomain. Hsueh's group, by hooking the 390 amino-terminal residues of the TSHr to the transmembrane segment of CD8 via a cleavable thrombin site, could prepare material displaying both TSAb and TSH binding activity (*26*). However, binding of TSH was only

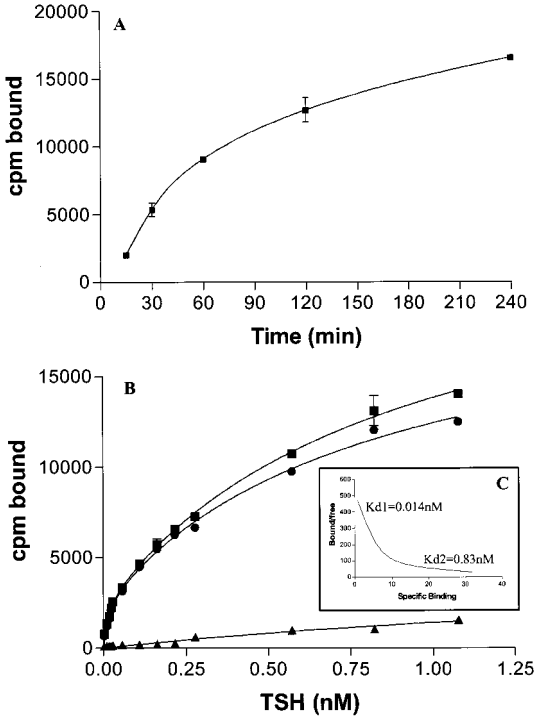

FIGURE 8: TSH binding on soluble ECD-10His. Binding of TSH on soluble ECD-10His was performed as described in Experimental Procedures. (A) Kinetics of binding. Sixty nanograms of soluble ECD-10His and 140 000 cpm of labeled TSH were incubated for 15−240 min. Unbound TSH was then removed by nickel agarose chromatography (see Experimental Procedures) and total cpm bound counted. (B) Saturation curve. Twenty nanograms of soluble ECD-10His was incubated for 4 h at room temperature with various concentrations of labeled TSH (nM). The concentration (nanomolar) of radiolabel specifically bound was calculated by subtracting from total binding nonspecific binding observed in the presence of 500 nM cold bTSH. Key: (■) total binding; (●) specific binding; (▲) nonspecific binding. (C) Scatchard analysis illustrating the two binding sites. All experiments were done in triplicate, and results are expressed as cpm bound. The data were analyzed with GraphPad Prism (GraphPad Software, Inc., San Diego, CA) which fits a two-site saturation binding curve.

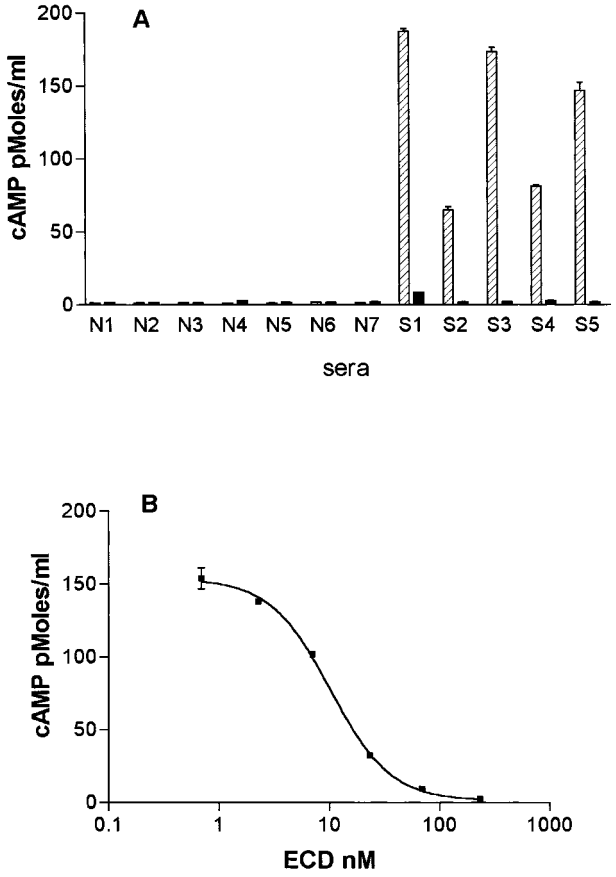

FIGURE 9: Neutralizing TSAb activity of the soluble ECD-10His. Soluble ECD-10His and sera from patients exhibiting a strong TSAb activity were incubated for 1 h at 37 °C in isotonic medium with CHO cells expressing the wild-type TSH receptor (JP26). cAMP produced by the cells was measured as described in Experimental Procedures. (A) Seven normal sera (N1−N7) and five sera with a TSAb activity (S1−S5) incubated with (black bars) or without (shaded bars) 3 μg of soluble ECD-10His. (B) Serum S1 incubated with various concentrations of soluble ECD-His. Duplicate samples were assayed in all experiments; results are expressed as picomoles of cAMP per milliliter. The data were analyzed with GraphPad Prism (GraphPad Software, Inc., San Diego, CA) which fits the data as a logistic model.

demonstrated by affinity labeling. Finally, Johnstone's group and our group succeeded in expressing large amounts of TSHr ectodomain at the surface of CHO cells via attachment of a glycosylphosphatidylinositol anchor (*30*). The ectodomain could be released by a specific GPI-PLC. It displayed TSAb neutralizing activity and, when stabilized by a monoclonal antibody, showed binding of labeled TSH in a PEG precipitation format (*30*).

In the present study, addition of a tag made of 10 histidine residues to the GPI-anchored TSHr ectodomain allowed to combine high expression at the surface of CHO cells (10^6 molecules capable of binding TSH/cell) and efficient purification. The capacity of GPI anchors to target large amounts of proteins to the plasma membrane is well exemplified by the situation in trypanosomes, the first organisms shown to use this strategy to make membrane proteins, in which a continuous mantle of GPI-anchored VSG proteins covers the whole cell (*42*). The possibility to release GPI-anchored molecules from the cell surface, by incubation with a GPI-specific PLC, makes it possible to obtain a TSHr ectodomain in a serum-free medium relatively poor in proteins. In comparison, production of a 261-residue His-tagged ectodomain via the normal secretory route required affinity chromatography on lectins prior to nickel−agarose chromatography, to avoid interference of serum proteins (*28*). The inclusion of 10 histidine residues in our tag, instead of the more "classical" 6-his tag, allowed elution from the cobalt−agarose column at higher imidazole concentrations, thus diminishing the amount of coeluted contaminant proteins. Also, it must be stressed that when compared with elution from immobilized mAbs, which involves drastic, potentially denaturing conditions, imidazole elution from cobalt−agarose columns is a particularly mild procedure. The procedure yielded 150 μg of highly purified ectodomain from 10^9 cells, i.e., about 10^6 molecules/cell.

The functional characteristics of the purified ectodomain deserves qualification. It allowed for the first time performance of direct TSH binding experiments with purified material. In previous experiments, stabilization of the ectodomain with the BA8 mAb was required in order to observe TSH binding (*30*). A variety of factors could explain this apparent discrepancy: in the previous experiments, commercial PI-PLC was used which, for reasons of economy, imposed to work in a very small volume and to detach cells

from the plastic surface before adding the enzyme. This treatment could induce partial degradation of the receptor, if not stabilized by the mAb. The use of "home-made" recombinant PI-PLC and a very efficient concentration module allowed working in larger volumes, which could avoid aggregation of the soluble ectodomain during the cleavage step. Also, the previous assay used PEG precipitation to measure binding of radiolabeled TSH; it is possible that inclusion of the BA8 mAb in the complex favored precipitation rather than improve the TSH binding. The new assay, using nickel-coated magnetic beads, displayed negligible nonspecific binding, which greatly improved sensitivity as compared with the PEG assay and allowed performance of classical saturation curves using purified ^{125}I-labeled TSH. Interestingly, these experiments provided evidence for two classes of TSH binding sites, both with an affinity higher than the one obtained from displacement curves using intact cells expressing the holoreceptor (JP19 cells) (see Figure 8). The site displaying the highest affinity (site A, $K_d = 0.014$ nM) represents only 13% of the total binding activity, which is mainly accounted for by site B ($K_d = 0.83$ nM). While the affinity of site B does not differ too much from that of the holoreceptor present on intact cells (0.83 versus 3.5 nM), it is more difficult to interpret the meaning of site A. One possibility would be that it corresponds to a fraction of receptors undergoing a structural alteration during the purification steps that increases their ability to bind TSH. Alternatively, we cannot exclude the possibility that this very high affinity would correspond to that of intact soluble ECD, the bulk of the material being partially degraded and showing lower affinity. The observation that only a fraction of the purified ECD (ca. 5%) is capable of binding TSH would fit with the idea that we are dealing with a heterogeneous population of molecules; some (the intact ECD?) would display very high affinity (site A); others, being partially degraded, would show a lower but still nanomolar affinity; still others (the majority) would be altered to the point of having lost the ability to bind TSH. One likely explanation for this functional heterogeneity is that purification of the ECD would lead to its partial denaturation, yielding molecules incapable of binding TSH. Against this hypothesis, however, we observed that the purified ECD resists several cycles of freeze−thaw (not shown). Also, the presence of the additional glycan moiety or of the His tag might affect the stability of the native structure. Similar difficulties in obtaining homogeneously functional material have been experienced with the truncated ECD261 and, very recently, ECD289 ectodomains (*28*, *43*). In this case, no TSH binding activity was present, but the ability to bind autoantibodies was both heterogeneous and unstable. Strategies to explore in order to improve the yield of the functional ectodomain may include the use of the BA8 or other mAbs or coproduction in the same cell of the ectodomain and the hormone. This strategy has proved efficient in the recent fruitful purification of a complex between hCG and the ectodomain of the CG/LH receptor (*7*).

It has been shown previously that ectodomain preparations incapable of binding TSH were perfectly able to neutralize TSAb or TBII from patients with Graves' disease (*28*, *44*). The common interpretation is that the epitopes of autoantibodies are less complex than the structures required for TSH binding. Not unexpectedly, the ectodomain prepared in the present study displayed also a very potent TSAb neutralizing activity. It was capable of inhibiting completely (>90%) stimulation of cAMP accumulation in JP26 cells (*36*) by a series of Graves' sera selected for their particularly strong TSAb activity. Titration experiments demonstrated that neutralization of 50% of the cAMP-stimulating activity of 50 μL of serum was achieved by 5 pmol (5 nM final concentration) of the ectodomain. This result was consistent with previous flow cytometry experiments (*30*, *45*) demonstrating low concentrations of TSAb in Graves' sera, as compared with blocking antibodies (TSBAb). It was also compatible with data obtained with the ECD261 (*28*). In this case, 50 ng (0.002 nmol; 8 nM final concentration) of the truncated ECD was able to neutralize the activity of a potent TBII. Assuming irreversible interaction (J. van Sande et al., to be published) and a 2:1 stoichiometry for the ECD−TSAb complex, both types of experiments indicate that the concentration of immunoglobulins with TSAb activity in patient's serum could reach 10 μg/mL (i.e., around 0.1% of total circulating immunoglobulins).

The suitability of the material for structural studies is exemplified by the direct analysis of glycosylation sites by mass spectrometry. The TSHr presents six potential sites of N-glycosylation. The difference between the molecular mass observed by SDS−PAGE before and after deglycosylation (∼115 vs ∼85 kDa for the mature holoreceptor; ∼55−60 vs ∼35−40 kDa for the α subunit) by the different groups working on this field (*46*−*53*) suggests that the majority, if not all, of these sites harbor glycan moieties. In a mass spectrometry study of the LH/CG receptor, it was shown recently that five potential N-glycosylation sites out of a total of six are effectively used (*54*). In the present study of the purified TSHr ectodomain, four residues corresponding to asparagines 77, 113, 198, and 302 were shown to harbor sugar moieties. Investigation of the two remaining sites will require further studies using different proteolytic enzymes to fragment the protein before MS analysis. Glycosylation of asparagine 302 confirmed previous results (*55*) showing decrease of molecular mass of the TSHr upon mutation of this residue. Direct demonstration that at least four potential N-glycosylation sites out of six are effectively glycosylated is in agreement with the presence in TSHr of more than 25 kDa of glycans, as observed by SDS−PAGE and western blotting of receptors present in transfected cells (*47*, *50*, *51*, *53*).

The availability of the purified ectodomain of the TSHr made in eukaryotic cells opens a series of new research avenues. Defining the interaction(s) between the ectodomain and the serpentine domain of the glycoprotein hormone receptors is crucial to our understanding of the mechanisms of activation of the receptors by hormones or autoantibodies. Now that both moieties are available, the ectodomain as a soluble protein and the serpentine domain as chimeric molecules essentially devoid of amino-terminal extension and inserted in the plasma membrane (our unpublished results), it will be possible to probe separately their structure−function relationships. Direct assay of the interactions between the ectodomain and the hormone or autoantibodies will be possible using the BIAcore technology. Similarly, biophysical assays such as circular dichroism or atomic force microscopy (AFM) will make it possible to determine the reliability of

the current model of the TSHr ectodomain, elaborated by analogy with the ribonuclease inhibitor.

ACKNOWLEDGMENT

We thank Veronique Janssens for expert technical assistance and Stephane Swillens for help with interpretation of the binding studies. We are grateful to BRAHMS diagnostics (Berlin, Germany) for providing radiolabeled bovine TSH and to Dr. O. Hayes Griffith (Institute of Molecular Biology, University of Oregon, Eugene, OR) for the kind gift of the PI-PLC expression plasmid.

REFERENCES

1. Parmentier, M., Libert, F., Maenhaut, C., Lefort, A., Gerard, C., Perret, J., Van Sande, J., Dumont, J. E., and Vassart, G. (1989) *Nucleic Acids Res. 17*, 10493−10493.
2. Libert, F., Lefort, A., Gerard, C., Parmentier, M., Perret, J., Ludgate, M., Dumont, J. E., and Vassart, G. (1989) *Biochem. Biophys. Res. Commun. 165*, 1250−1255.
3. Tominaga, T., Yamashita, S., Nagayama, Y., Morita, S., Yokoyama, N., Izumi, M., and Nagataki, S. (1991) *Acta Endocrinol. 124*, 290−294.
4. Kajava, A. V., Vassart, G., and Wodak, S. J. (1995) *Structure 3*, 867−877.
5. Jiang, X., Dreano, M., Buckler, D. R., Cheng, S., Ythier, A., Wu, H., Hendrickson, W. A., and el Tayar, N. (1995) *Structure 3*, 1341−1353.
6. Kobe, B., and Deisenhofer, J. (1993) *Nature 366*, 751−756.
7. Remy, J. J., Nespoulous, C., Grosclaude, J., Grebert, D., Couture, L., Pajot, E., and Salesse, R. (2001) *J. Biol. Chem. 276*, 1681−1687.
8. Kunishima, N., Shimada, Y., Tsuji, Y., Sato, T., Yamamoto, M., Kumasaka, T., Nakanishi, S., Jingami, H., and Morikawa, K. (2000) *Nature 407*, 971−977.
9. Zhang, M., Tong, K. P., Fremont, V., Chen, J., Narayan, P., Puett, D., Weintraub, B. D., and Szkudlinski, M. W. (2000) *Endocrinology 141*, 3514−3517.
10. Duprez, L., Parma, J., Costagliola, S., Hermans, J., Van Sande, J., Dumont, J. E., and Vassart, G. (1997) *FEBS Lett. 409*, 469−474.
11. Vassart, G. (1997) *Horm. Res. 48* (Suppl. 4), 47−50.
12. Rees Smith, B., McLachlan, S. M., and Furmaniak, J. (1988) *Endocr. Rev. 9*, 106−121.
13. Morgenthaler, N. G., Tremble, J., Huang, G., Scherbaum, W. A., McGregor, A. M., and Banga, J. P. (1996) *J. Clin. Endocrinol. Metab. 81*, 700−706.
14. Prentice, L., Sanders, J. F., Perez, M., Kato, R., Sawicka, J., Oda, Y., Jaskolski, D., Furmaniak, J., and Smith, B. R. (1997) *J. Clin. Endocrinol. Metab. 82*, 1288−1292.
15. Segaloff, D. L., and Ascoli, M. (1993) *Endocr. Rev. 14*, 324−347.
16. Graves, P. N., Vlase, H., and Davies, T. F. (1995) *Endocrinology 136*, 521−527.
17. Costagliola, S., Alcalde, L., Ruf, J., Vassart, G., and Ludgate, M. (1994) *J. Mol. Endocrinol. 13*, 11−21.
18. Harfst, E., Johnstone, A. P., and Nussey, S. S. (1992) *J. Mol. Endocrinol. 9*, 227−236.
19. Costagliola, S., Alcade, L., Ruf, J., Vassart, G., and Ludgate, M. (1994) *J. Mol. Endocrinol. 13*, 11−21.
20. Seetharamaiah, G. S., Desai, R. K., Dallas, J. S., Tahara, K., Kohn, L. D., and Prabhakar, B. S. (1993) *Autoimmunity 14*, 315−320.
21. Huang, G. C., Page, M. J., Nicholson, L. B., Collison, K. S., McGregor, A. M., and Banga, J. P. (1993) *J. Mol. Endocrinol. 10*, 127−142.
22. Chazenbalk, G. D., and Rapoport, B. (1995) *J. Biol. Chem. 270*, 1543−1549.
23. Vlase, H., Graves, P. N., Magnusson, R. P., and Davies, T. F. (1995) *J. Clin. Endocrinol. Metab. 80*, 46−53.
24. Harfst, E., Johnstone, A. P., and Nussey, S. S. (1992) *Lancet 339*, 193−194.
25. Rapoport, B., McLachlan, S. M., Kakinuma, A., and Chazenbalk, G. D. (1996) *J. Clin. Endocrinol. Metab. 81*, 2525−2533.
26. Osuga, Y., Liang, S. G., Dallas, J. S., Wang, C., and Hsueh, A. J. (1998) *Endocrinology 139*, 671−676.
27. Osuga, Y., Kudo, M., Kaipia, A., Kobilka, B., and Hsueh, A. J. (1997) *Mol. Endocrinol. 11*, 1659−1668.
28. Chazenbalk, G. D., Jaume, J. C., McLachlan, S. M., and Rapoport, B. (1997) *J. Biol. Chem. 272*, 18959−18965.
29. Da Costa, C. R., and Johnstone, A. P. (1998) *J. Biol. Chem. 273*, 11874−11880.
30. Costagliola, S., Khoo, D., and Vassart, G. (1998) *FEBS Lett. 436*, 427−433.
31. Lee, M. H., Park, J. Y., Cho, B. Y., and Chae, C. B. (1999) *J. Clin. Endocrinol. Metab. 84*, 1391−1397.
32. Costagliola, S., Rodien, P., Many, M. C., Ludgate, M., and Vassart, G. (1998) *J. Immunol. 160*, 1458−1465.
33. Bernasconi, E., Fasel, N., and Wittek, R. (1996) *J. Cell Sci. 109*, 1195−1201.
34. Koke, J. A., Yang, M., Henner, D. J., Volwerk, J. J., and Griffith, O. H. (1991) *Protein Expression Purif. 2*, 51−58.
35. Bush, G. L., Tassin, A. M., Friden, H., and Meyer, D. I. (1991) *J. Biol. Chem. 266*, 13811−13814.
36. Perret, J., Ludgate, M., Libert, F., Gerard, C., Dumont, J. E., Vassart, G., and Parmentier, M. (1990) *Biochem. Biophys. Res. Commun. 171*, 1044−1050.
37. Brooker, G., Harper, J. F., Terasaki, W. L., and Moylan, R. D. (1979) *Adv. Cyclic Nucleotide Res. 10*, 1−33.
38. Shevchenko, A., Wilm, M., Vorm, O., and Mann, M. (1996) *Anal. Chem. 68*, 850−858.
39. Jensen, O. N., Podtelejnikov, A., and Mann, M. (1996) *Rapid Commun. Mass Spectrom. 10*, 1371−1378.
40. Wilm, M., and Mann, M. (1996) *Anal. Chem. 68*, 1−8.
41. Harfst, E., Johnstone, A. P., and Nussey, S. S. (1992) *Lancet 339*, 193−194.
42. Ferguson, M. A., Brimacombe, J. S., Cottaz, S., Field, R. A., Guther, L. S., Homans, S. W., McConville, M. J., Mehlert, A., Milne, K. G., and Ralton, J. E. (1994) *Parasitology 108* (Suppl.), S45−S54.
43. Chazenbalk, G. D., McLachlan, S. M., Pichurin, P., Yan, X. M., and Rapoport, B. (2001) *J. Clin. Endocrinol. Metab. 86*, 1287−1293.
44. Seetharamaiah, G. S., Dallas, J. S., Patibandla, S. A., Thotakura, N. R., and Prabhakar, B. S. (1997) *J. Immunol. 158*, 2798−2804.
45. Jaume, J. C., Kakinuma, A., Chazenbalk, G. D., Rapoport, B., and McLachlan, S. M. (1997) *J. Clin. Endocrinol. Metab. 82*, 500−507.
46. Loosfelt, H., Pichon, C., Jolivet, A., Misrahi, M., Caillou, B., Jamous, M., Vannier, B., and Milgrom, E. (1992) *Proc. Natl. Acad. Sci. U.S.A. 89*, 3765−3769.
47. Misrahi, M., Ghinea, N., Sar, S., Saunier, B., Jolivet, A., Loosfelt, H., Cerutti, M., Devauchelle, G., and Milgrom, E. (1994) *Eur. J. Biochem. 222*, 711−719.
48. Graves, P. N., Vlase, H., Bobovnikova, Y., and Davies, T. F. (1996) *Endocrinology 137*, 3915−3920.
49. Kohn, L. D., Shimura, H., Shimura, Y., Hidaka, A., Giuliani, C., Napolitano, G., Ohmori, M., Laglia, G., and Saji, M. (1995) *Vitam. Horm. 50*, 287−384.
50. Chazenbalk, G. D., Tanaka, K., Nagayama, Y., Kakinuma, A., Jaume, J. C., McLachlan, S. M., and Rapoport, B. (1997) *Endocrinology 138*, 2893−2899.

51. Oda, Y., Sanders, J., Roberts, S., Maruyama, M., Kiddie, A., Furmaniak, J., and Smith, B. R. (1999) *J. Clin. Endocrinol. Metab. 84*, 2119−2125.
52. Nagayama, Y., Nishihara, E., Namba, H., Yamashita, S., and Niwa, M. (2000) *J. Pharmacol. Exp. Ther. 295*, 404−409.
53. Siffroi-Fernandez, S., Costagliola, S., Paumel, S., Giraud, A., Banga, J. P., and Franc, J. L. (2001) *Biochem. J. 354*, 331−336.
54. Vu-Hai, M. T., Huet, J. C., Echasserieau, K., Bidart, J. M., Floiras, C., Pernollet, J. C., and Milgrom, E. (2000) *Biochemistry 39*, 5509−5517.
55. Tanaka, K., Chazenbalk, G. D., McLachlan, S. M., and Rapoport, B. (1998) *J. Biol. Chem. 273*, 1959−1963.

BI0107389